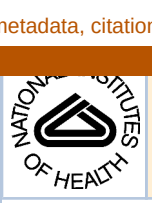

Published in final edited form as:

J Infect Dis. 2010 March 15; 201(6): 946–955. doi:10.1086/651022.

Escape from Human Monoclonal Antibody Neutralization Affects In Vitro and In Vivo Fitness of Severe Acute Respiratory Syndrome Coronavirus

Barry Rockx[1,3], **Eric Donaldson**[1], **Matthew Frieman**[1], **Timothy Sheahan**[1], **Davide Corti**[4], **Antonio Lanzavecchia**[4], and **Ralph S. Baric**[1]

[1] Department of Epidemiology, University of North Carolina, Chapel Hill, North Carolina [2] Department of Microbiology and Immunology, University of North Carolina, Chapel Hill, North Carolina [3] Rocky Mountain Laboratories, NIAID, NIH, Hamilton, Montana [4] Institute for Research in Biomedicine, Bellinzona, Switzerland

Abstract

Background—Severe Acute Respiratory Syndrome (SARS) emerged as a human disease in 2002 and detailed phylogenetic analysis and epidemiological studies have suggested that the SARS-Coronavirus (SARS-CoV) originated from animals. The Spike (S) glycoprotein has been identified as a major target of protective immunity and contains at least three regions that are targeted by neutralizing antibodies in the S1 and S2 domains. We previously characterized a panel of neutralizing human monoclonal antibodies (MAbs) but the majority of epitopes recognized by the MAbs remained unknown.

Methods—In this study we generated neutralization escape mutants and studied the effect of these neutralization escape mutations on human and animal receptor usage as well as in vitro and in vivo fitness.

Results—Distinct but partially overlapping sets of amino acids were identified that are critical to the binding of MAbs with differential neutralization profiles. We also identified possible interactions between the S1 and S2 domains of the SARS-CoV S glycoprotein. Finally, we showed that escape from neutralization usually attenuates SARS-CoV infection.

Conclusions—These data provide a mechanism to overcome neutralization escape by using broadly cross reactive cocktails of cross-neutralizing MAbs that recognize residues within the receptor binding domain, critical for virus replication and virulence.

Keywords

SARS-CoV; neutralization escape; viral fitness; monoclonal antibody

Introduction

Severe acute respiratory syndrome coronavirus (SARS-CoV) emerged in 2002/2003, infecting over 8000 people with an 11% fatality rate [1]. SARS-CoV is a new member of the virus family

Corresponding author: Ralph S. Baric Department of Epidemiology, University of North Carolina, Campus Box 7435, Chapel Hill, North Carolina. T: 919-966-3895.

Conflict of interest: The authors declare no conflict of interest.

Coronaviridae that likely emerged from strains that are continually circulating in bats and other animals sold in wet markets. Thus, vaccines and therapeutics must target a heterogeneous pool of human and zoonotic variants to preserve the public health.

Several studies have shown that the SARS-CoV Spike (S) glycoprotein binds the ACE2 receptor and is a major component of protective immunity. It contains at least three domains that are targeted by neutralizing antibodies. We previously generated and characterized a panel of 23 human MAbs that neutralized one or multiple homologous and heterologous SARS-CoV S glycoprotein variants [2]. These MAbs could be categorized into 6 different neutralization profiles based on their ability to neutralize isogenic SARS-CoVs bearing different human and zoonotic S glycoproteins [2]. Groups I through III MAbs only neutralized human strains but not the zoonotic strains and group VI comprised of four MAbs that could neutralize all human and zoonotic SARS-CoV strains tested in vitro and in vivo. We demonstrated that these MAbs are attractive candidates for prophylactic treatment for the prevention of laboratory-acquired infections as well as zoonotic introductions [2]. However, escape from neutralization is a concern when developing these MAbs for therapeutics.

In the present study we generated neutralization escape mutants for a panel of 11 human MAbs. Using structural analysis and cross-neutralization assays, several distinct sets of residues critical for neutralization were identified as well as a novel site outside the RBD that is likely involved in receptor interaction. In addition the effects of these mutations on the fitness and virulence of SARS-CoV were determined in vitro and in vivo. These data identify subsets of compatible cocktails of human MAbs that could serve as potential therapeutic agents in laboratory exposures and/or in new SARS-CoV outbreak settings.

Materials and Methods

Viruses and cells

Recombinant icUrbani, icGZ02 and icHC/SZ/61/03 and all derived escape mutants were propagated on Vero E6 cells as previously described [2-3]. Delayed brain tumor (DBT) cells stably expressing human (h) or civet (c) ACE2 were isolated by flow cytometry as previously described [3].

Growth curves were performed by inoculating Vero E6, DBT-hACE2 and DBT-cACE2 cell cultures with the different viruses at a MOI of 0.1 for 1h and overlaid with medium. Virus samples were collected at various time points post infection and stored at −70°C until viral titers were determined by plaque assay as previously described [2-3].

Escape mutant analysis

Human MAbs against SARS-CoV were generated as described previously [4]. Neutralization resistant SARS-CoV mutants were generated as described previously [2]. Briefly, 1×10^6 pfu of icUrbani was incubated with 30μg of a neutralizing MAb in 100 μl media for 1 h at 37°C and then inoculated onto 10^6 Vero E6 cells in the presence of the respective MAb at the same concentration. The icHC/SZ/61/03 isolate was used for generating a neutralization escape mutant for MAb S227.14, as several attempts to generate escape mutants from this antibody using icUrbani and icGZ02 proved unsuccessful. The development of cytopathic effect (CPE) was monitored over 72 h and progeny viruses harvested. MAb treatment was repeated two additional times, passage 3 viruses were plaque purified in the presence of MAb and neutralization resistant viruses were isolated. Experiments were performed in duplicate and the S glycoprotein gene of individual plaques from each experiment was sequenced as previously described [2]. The neutralization titers between wild type and MAb resistant viruses were determined as previously described [2].

Computer modeling of RBD interactions with hACE2, mACE2 and cACE2

The crystal structure coordinates of SARS-CoV RBD interacting with the human ACE2 receptor (PDB code 2AJF, Chain A and Chain E) were used as a template to map the location of the a.a. changes identified in the escape mutants.

Mouse infection

Female BALB/cBy mice (12-month-old from National Institute on Aging,) were intranasally inoculated with 5.0×10^5 pfu (icUrbani and its escape mutants) or 10^5 pfu (icGZ02, icHC/SZ/61/03 and their respective escape mutants) of virus in a 50μl volume as previously described [2-3,5]. Mice were weighed daily and four or five days post infection lungs were removed and frozen at −70°C for determination of viral titers and histopathologic changes as described previously [2-3]. Experimental protocols were reviewed and approved by the Institutional Animal Care and Use Committee at UNC Chapel Hill.

Results

Identification of amino acids critical for virus neutralization

The icUrbani isolate was used to generate neutralization escape mutants. Based on neutralization patterns across the groups, we selected the group I MAb: S228.11; two group II MAbs: S111.7 and S224.17; two group III MAbs: S3.1 and S127.6; two group IV MAbs: S110.4 and S231.19 and all four group VI broadly cross neutralizing MAbs: S109.8, S215.17, S227.14 and S230.15.

Importantly, ten out of eleven escape mutants contained single a.a. changes whereas the S3.1 escape mutant contained two a.a. changes at positions L443R and Y777D (Table 1). The S109.8 escape mutant contained a single T332I change, while the S230.15 escape mutant contained a L443R change identical to what was previously shown using the S glycoprotein from the early phase icGZ02 isolate [2]. Interestingly, several MAb escape mutants from different neutralization groups had a.a. changes in common (Table 1). The a.a. change associated with neutralization escape from S127.6 was a D480Y mutation, which was previously shown to decrease the neutralization efficacy of the 80R MAb [6]. The group I MAb S228.11, group IV MAb S110.4 and the group VI MAb S215.17 all selected for escape mutant viruses with an a.a. change at position 462. Finally, the generation of a MAb neutralization escape variant using MAb S227.14 was unsuccessful even after several attempts using both the icGZ02 [2] and icUrbani isolate. However using the icHC/SZ/61/03 isolate, two MAb neutralization escape mutants were isolated which contained a single amino acid mutation at position 390, resulting in either a K390Q or K390E change.

Cross-neutralization of MAb neutralization escape mutants

Identification of mutations associated with neutralization escape yielded a complex set of overlapping or nearly overlapping mutations within the RBD, suggesting that escape mutants selected with one antibody may provide resistance to neutralization using other human MAbs. Consequently, we examined the cross neutralization patterns of the escape mutants using the panel of select MAbs (Figure 1). The neutralization efficacy of the group I MAb S228.11 was not only ablated by the P462A change present in its respective escape mutant, but also could not neutralize viruses containing mutations at L443R, F460C, P462H and Y777D (Figure 1A). Neutralization efficacy of the two group II MAbs S111.7 and S224.1 was ablated for all other escape mutants with the exception of the T332I and D480Y mutants (Figure 1B). Neutralization efficacy of the group III MAb S127.6 was not affected by any a.a. change other than the D480Y change that was selected for in its respective escape mutant. In contrast, neutralization by the other group III MAb S3.1 was ablated by its respective escape mutations L443R and Y777D

as well as mutations F460C and P462H (Figure 1C). MAb neutralization escape mutants generated against the group IV MAbs (S110.4 and S231.2) contained two a.a. changes located closely together (F460C and P462H). Not surprising, the neutralization efficacies for these two MAbs was very similar (Figure 1D). Finally, the group VI MAbs were previously identified to cross-neutralize all human and zoonotic SARS-CoV isolates unaffected by the a.a. changes naturally occurring during the SARS-CoV epidemic [2]. MAbs S109.8 and S230.15 were only affected by the mutations that were present in their respective neutralization escape mutants (e.g. T332I and L443R) (Figure 1E). Neutralization by S215.17 was affected by a.a. changes L443R, F460C and P462H but not by Y777D. This was surprising as MAb S110.4, which selected for the identical P462H mutant as well as MAb 228.11, which selected for mutation P462A, were both affected by all 4 a.a. changes (L443R, F460C, P462H and Y777D). None of the a.a. changes generated in the other escape mutants affected the neutralization efficacy of S227.14.

Structural mapping of amino acids critical for neutralization

The structure of the SARS-CoV RBD complexed with ACE2, was recently resolved allowing us to map the locations of the a.a. changes onto the RBD structure [7]. As previously shown, a.a. 332 of the RBD is critical for neutralization by MAb S109.8 and located on the side of the RBD in a loop that is not in direct contact with the receptor, ACE2 (Figure 2). Interestingly, while MAbs S228.1, S224.17, S3.1, S110.4, S231.9, S215.17 and S230.15 recognize distinct antigenic groups based on their neutralizing profiles of isogenic viruses with variant S glycoproteins, the locations of the a.a. changes associated with neutralization escape map within 4 ångstrom of each other (Figure 2). Unfortunately the location of the a.a. 777 alteration is downstream of the RBD and upstream of the heptad repeat region and therefore no structural information was available. The D480Y change is likely part of or influencing presentation of a distinct epitope recognized by MAb S127.6, belonging to group III (Figure 2). Neutralization by the cross-neutralizing MAb S227.14 was not affected by any of the mutations generated by the other MAbs. The cross-neutralization data suggests that the a.a. change K390Q/E associated with MAb neutralization escape from S227.14 is uniquely separate from other escape mutants (Figure 2).

Effect of S glycoprotein mutations on in vitro growth

The Urbani S glycoprotein RBD is critical for docking and entry and engages both human and civet ACE2 receptors [8-9]. All but one of the neutralization-escape mutations (D463G) are either directly adjacent (L443R) or within four Ångstrom (K390Q/E, F460C, P462A/H, D463G and D480Y) of key contact residue sites encoded in the RBD at positions 436, 442, 473, 475, 479 and 491 [7], which may interfere with binding to human or civet ACE2. All neutralization escape viruses grew efficiently in Vero E6 cells reaching comparable peak titers between 10^7 and 10^8 pfu/ml by 36 hours post infection (h.p.i.) (Figure 3A). Replication of all viruses was delayed early in infection as shown by a one to two log reduction of titer at 12 h.p.i as compared to the wild type icUrbani, with the exception of the escape mutant with a P462H change (2-way ANOVA; $p<0.05$). A similar trend was seen in DBT cells expressing the human ACE2 molecule (Figure 3B). Growth in DBT cells expressing the civet ACE2 molecule was affected by all a.a. changes tested. All viruses, with the exception of the F460C mutant, reached peak titers of ~10^7 pfu/ml but were delayed 12 h.p.i. in replication as compared to icUrbani (Figure 3C). Importantly at 36 h.p.i. the escape mutant virus with a change at F460C showed a 2 log reduction of titer as compared to icUrbani (2-way ANOVA; $p<0.01$) suggesting that some escape mutations may alter virus fitness in cACE2 expressing DBT cells; potentially hampering virus persistence in animal reservoirs.

Effect of S glycoprotein mutations on in vivo growth

Mutations within the S glycoprotein of SARS-CoV can potentially alter morbidity and mortality [3], so to test this possibility 12-month-old BALB/c mice were inoculated with either wild type icUrbani, icGZ02, icHC/SZ/61/03 and each of their respective neutralization escape mutants. Under these conditions, icUrbani resulted in ~15% weight loss phenotype. Interestingly, while the Y777D change had an attenuating effect on in vitro growth, no difference in weight loss could be detected as compared with the icUrbani isolate (Figure 4A). In contrast, neutralization-escape viruses with a D480Y or D463G changes were attenuated with infected mice losing only 5% of their weight by day 4 p.i. while viruses with a T332I, L443R, F460C or P462H a.a. change were completely attenuated in aged animals (Figure 4A). Viral titers in the lungs of infected animals at day 5 p.i. did not correlate completely with weight loss as previously seen [5]. The P462H mutant virus grew to comparable titers as icUrbani (10^6 pfu/gr; Figure 4B). However, T332I, F460C and L443R mutant virus titers were significantly reduced 1, 2 and 4 logs respectively, as compared to icUrbani. In agreement with this data the T332I and L443R mutations generated in icGZ02 previously [2], were also completely attenuated in aged mice (data not shown). The K390E/Q mutants using the icHC/SZ/61/03 strain associated with neutralization-escape from MAb S227.14 were completely attenuated in aged mice with no loss of weight whereas the WT icHC/SZ/61/03 infected mice lost up to 20% of their weight by day 4 post-infection and 2 out 5 died (Figure 4C). Interestingly no difference in virus titers was observed at day 4 post infection between the WT and neutralization escape mutants of the icHC/SZ/61/03 (Figure 4D).

In agreement with the observed weight loss in animals infected with the 2 lethal strains (icGZ02 and icHC/SZ/61/03), by 4 days p.i. a necrotizing bronchiolitis could be observed in the lungs of these 12-month-old mice, with marked loss and/or attenuation of the bronchiolar epithelium (Fig. 5). This was accompanied by widespread injury of the alveolar parenchyma. The histopathology of this injury to the gas exchange region of the lung consisted of diffuse alveolar damage, interstitial edema, and hyaline membrane formation. Interestingly in animals infected with the neutralization escape mutants generated against the cross-neutralizing MAbs S109.8, S230.15 and S227.14, had minimal or no alveolitis present in the pulmonary parenchyma at 4 d.p.i. and no hyaline membranes were observed (Fig. 5).

Discussion

Neutralizing antibodies have been shown to be important in the recovery and protection against infectious diseases. However, the high mutation rate and heterogeneity of viruses is a major problem in developing therapeutic MAbs, especially against human viruses which emerge from heterogeneous pools circulating in animal reservoirs. To our knowledge effects of escape mutations of human MAbs following acute infection with human epidemic and zoonotic strains of an emerging virus have not been rigorously investigated.

The goal of this study was to characterize the antibody targeting specificity of a large panel of neutralizing human MAbs and identifying residues that are critical to neutralization of SARS-CoV through isolation of escape mutants. The effects of these mutations on cross neutralization, receptor usage and in vitro and in vivo replication were determined with the goal of identifying compatible candidate cocktails of broad spectrum neutralizing antibody therapeutics for the treatment of future SARS-CoV epidemics. We identified the presence of several critical residues associated with neutralization escape from 11 MAbs that showed overlap. In addition, we showed that mutations associated with MAb neutralization escape also affected the kinetics of replication in vitro and the degree of pathogenicity in mice.

SARS-CoV is an excellent model system to study the development of therapeutic antibodies against an emerging virus. SARS-CoV, like other RNA-viruses, has a high mutation rate which

was important for adapting to changing environments like cross-species transmission [8,11]. Using a panel of recombinant viruses bearing different S glycoproteins from human epidemic and animal strains, we previously characterized a panel of human MAbs and described six distinct neutralization profiles suggesting the presence of several putative conformational epitopes [2].

In this manuscript, a detailed analysis was performed of the residues critical for neutralization by 11 different human MAbs that differentially neutralized animal and human strains. Four of these residues at positions 443, 460, 462 and 463 map within five ångstroms in the RBD structure and were associated with escape from neutralization with MAbs from the five different neutralization profiles, suggesting overlapping antigenic sites. While MAb-RBD co-crystallization studies will be necessary to determine the complex architecture and orientation of the RBD neutralizing epitopes, our data suggest that subtle changes in and around the escape mutation site can impact antibody binding and neutralization. In fact, experimental and structural data is available that supports our hypothesis of overlapping epitopes on the SARS-CoV RBD, recognized by MAbs that display distinct neutralization profiles [12-16].

Escape mutant analysis has assisted in the identification of antigenic sites for several viruses including Rhinovirus and SARS-CoV [17-21] and has been used previously to identify the importance of P462 in the neutralization of SARS-CoV by MAb CR3014 [21]. The structures of two MAbs complexed with the SARS-CoV RBD have been previously described [15-16]. The MAb m396 mainly recognizes a 10-residue (482-491) loop that protrudes from the RBD surface and competed with S230.15 for binding to the RBD [22]. Since the S230.15 epitope includes the 443 residue that is distant from the m396 epitope, competition likely occurs through steric hindrance between the two MAbs. The 80R MAb was found to interact with 29 residues between 426 and 492 on the SARS-CoV RBD. The D480 residue was of particular interest as mutations at this residue completely abolished binding to 80R. Interestingly, a mutation at residue 480 was also found to affect the neutralization efficacy of one of the group III MAbs described in this study (S127.6), suggesting that these MAbs recognize an identical or overlapping epitope as previously hypothesized [18].

The cross-neutralization data suggested a link between residue Y777 and one or more groups of residues at locations L443, F460, P462 and D463. Recently another study has shown a relationship between a.a. changes in the S1 and S2 domains of SARS-CoV, affecting neutralization [17]. Currently the structure of the complete SARS-CoV S glycoprotein bound to its receptor ACE2 has not been elucidated and therefore mapping the effects of long-range a.a. changes outside the RBD on the global S glycoprotein structure are not possible. However, these data suggest that the S1 and S2 domains of the S glycoprotein communicate with the RBD and may even interact physically in the higher-order structure of the S glycoprotein as has been shown for other coronaviruses [23-24]. Importantly, other domains outside the RBD have been targeted by neutralizing MAbs, including the a.a. 130-140 and HR-2 [25]. Although it is not clear whether these domains are linked with the RBD, our previous work also implicated changes at positions 132 and 228 as affecting MAbs S132 and S228.11 neutralization after RBD binding [2].

While the generation of neutralization escape mutants can be a very helpful tool in the identification of residues critical for neutralization, it generally compromises the use of these single MAbs as prophylaxis or treatment. However, a.a. changes within the SARS-CoV S glycoprotein not only affect neutralization but can also have dramatic effects on fitness and virulence of the virus. We previously showed that a single mutation at position 577 or 578 outside the RBD in some zoonotic S glycoprotein genes, was associated with the development of CPE in cell culture [3]. In addition, the introduction of 6 a.a. changes in the SARS-CoV S glycoprotein resulted in lethal infection of aged mice [3]. In the current study we show a clear

effect by several different escape a.a. mutations on in vitro replication. Since many of the escape mutants grew to similar titers with an initial delay in growth, the observed mutations likely mediate a reduced RBD affinity for the hACE2 receptor resulting in a delay of entry. Some also influenced the ability of virus to grow in cells expressing civet ACE2 suggesting that these escape viruses may be inefficiently maintained in animal reservoirs. Encouragingly, many escape mutations also had a clear effect on in vivo pathogenesis using an aged mouse model. Although a mutation at residue 777 did not affect in vivo pathogenesis, all other mutations either partially or completely attenuated SARS-CoV infection in aged mice. A decrease in virulence of neutralization escape mutants has also been observed with H5 and H9 influenza viruses and coincided with reduced affinity of the mutant HA for it's receptor [26-27]. Given the delayed growth of many of these escape mutants on cells expressing hACE2, we anticipate that they would be attenuated in humans. In addition, we were unsuccessful in isolating mutants resistant to the sequential generation of escape variants using different MAbs. Several attempts to rescue virus from escape mutants that were incubated with other neutralizing MAbs in the presence of the original MAb were unsuccessful (unpublished data). Therefore a cocktail of potent broadly cross-neutralizing MAbs, like the one previously described [2], will overcome neutralization escape and provide protection from disease after laboratory accidents, zoonotic introductions or focal outbreaks of disease [18,28].

In conclusion, our data support the hypothesis that multiple overlapping neutralizing epitopes exist within the RBD of the SARS-CoV S glycoprotein with clusters of escape mutations affecting neutralization by MAbs with different neutralization profiles. A residue at location 777, associated with epitopes involving residues 443, 460, 462 and 463, suggests long range interactions within the SARS-CoV S glycoprotein. We showed that neutralization escape comes with the cost of reduced viral fitness and propose the development of a broadly cross-neutralizing MAb cocktail to overcome the generation of escape variants. We propose that a cocktail of MAbs S227.14 and S230.15 is particularly robust as they individually neutralize a broad panel of human and zoonotic SARS-CoV variants, select for escape mutations at different sites in the RBD and escape mutants are severely attenuated in aged animals.

Acknowledgments

This work was supported by NIH NIAID grants P01-AI059443 and AI059136 and by the European Union SARSVAC grant N. SP22.CT.2004.511065.

Financial support: This work was supported by NIH NIAID grants P01-AI059443 and AI059136 R.B. and by the European Union SARSVAC grant N. SP22.CT.2004.511065 A.L.

References

1. Chan-Yeung M, Xu RH. SARS: epidemiology. Respirology 2003;8(Suppl):S9–14. [PubMed: 15018127]
2. Rockx B, Corti D, Donaldson E, et al. Structural basis for potent cross-neutralizing human monoclonal antibody protection against lethal human and zoonotic severe acute respiratory syndrome coronavirus challenge. J Virol 2008;82:3220–35. [PubMed: 18199635]
3. Rockx B, Sheahan T, Donaldson E, et al. Synthetic reconstruction of zoonotic and early human severe acute respiratory syndrome coronavirus isolates that produce fatal disease in aged mice. J Virol 2007;81:7410–23. [PubMed: 17507479]
4. Traggiai E, Becker S, Subbarao K, et al. An efficient method to make human monoclonal antibodies from memory B cells: potent neutralization of SARS coronavirus. Nat Med 2004;10:871–5. [PubMed: 15247913]
5. Rockx B, Baas T, Zornetzer GA, et al. Early Upregulation of ARDS Associated Cytokines Promote Lethal Disease in an Aged Mouse Model of SARS-CoV Infection. J Virol. 2009

6. Sui J, Li W, Roberts A, et al. Evaluation of human monoclonal antibody 80R for immunoprophylaxis of severe acute respiratory syndrome by an animal study, epitope mapping, and analysis of spike variants. J Virol 2005;79:5900–6. [PubMed: 15857975]
7. Li F, Li W, Farzan M, Harrison SC. Structure of SARS coronavirus spike receptor-binding domain complexed with receptor. Science 2005;309:1864–8. [PubMed: 16166518]
8. Li W, Zhang C, Sui J, et al. Receptor and viral determinants of SARS-coronavirus adaptation to human ACE2. Embo J 2005;24:1634–43. [PubMed: 15791205]
9. Sheahan T, Rockx B, Donaldson E, Corti D, Baric R. Pathways of cross-species transmission of synthetically reconstructed zoonotic severe acute respiratory syndrome coronavirus. J Virol 2008;82:8721–32. [PubMed: 18579604]
10. Groothuis JR, Simoes EA, Levin MJ, et al. Prophylactic administration of respiratory syncytial virus immune globulin to high-risk infants and young children. The Respiratory Syncytial Virus Immune Globulin Study Group. N Engl J Med 1993;329:1524–30. [PubMed: 8413475]
11. Kan B, Wang M, Jing H, et al. Molecular evolution analysis and geographic investigation of severe acute respiratory syndrome coronavirus-like virus in palm civets at an animal market and on farms. J Virol 2005;79:11892–900. [PubMed: 16140765]
12. Pak JE, Sharon C, Satkunarajah M, et al. Structural Insights into Immune Recognition of the Severe Acute Respiratory Syndrome Coronavirus S Protein Receptor Binding Domain. J Mol Biol. 2009
13. Bian C, Zhang X, Cai X, et al. Conserved amino acids W423 and N424 in receptor-binding domain of SARS-CoV are potential targets for therapeutic monoclonal antibody. Virology 2009;383:39–46. [PubMed: 18986662]
14. He Y, Lu H, Siddiqui P, Zhou Y, Jiang S. Receptor-binding domain of severe acute respiratory syndrome coronavirus spike protein contains multiple conformation-dependent epitopes that induce highly potent neutralizing antibodies. J Immunol 2005;174:4908–15. [PubMed: 15814718]
15. Hwang WC, Lin Y, Santelli E, et al. Structural basis of neutralization by a human anti-severe acute respiratory syndrome spike protein antibody, 80R. J Biol Chem 2006;281:34610–6. [PubMed: 16954221]
16. Prabakaran P, Gan J, Feng Y, et al. Structure of severe acute respiratory syndrome coronavirus receptor-binding domain complexed with neutralizing antibody. J Biol Chem 2006;281:15829–36. [PubMed: 16597622]
17. Mitsuki YY, Ohnishi K, Takagi H, et al. A single amino acid substitution in the S1 and S2 Spike protein domains determines the neutralization escape phenotype of SARS-CoV. Microbes Infect 2008;10:908–15. [PubMed: 18606245]
18. Sui J, Aird DR, Tamin A, et al. Broadening of neutralization activity to directly block a dominant antibody-driven SARS-coronavirus evolution pathway. PLoS Pathog 2008;4:e1000197. [PubMed: 18989460]
19. Bizebard T, Barbey-Martin C, Fleury D, et al. Structural studies on viral escape from antibody neutralization. Curr Top Microbiol Immunol 2001;260:55–64. [PubMed: 11443881]
20. Sherry B, Mosser AG, Colonno RJ, Rueckert RR. Use of monoclonal antibodies to identify four neutralization immunogens on a common cold picornavirus, human rhinovirus 14. J Virol 1986;57:246–57. [PubMed: 2416951]
21. ter Meulen J, van den Brink EN, Poon LL, et al. Human monoclonal antibody combination against SARS coronavirus: synergy and coverage of escape mutants. PLoS Med 2006;3:e237. [PubMed: 16796401]
22. Zhu Z, Chakraborti S, He Y, et al. Potent cross-reactive neutralization of SARS coronavirus isolates by human monoclonal antibodies. Proc Natl Acad Sci U S A. 2007
23. McRoy WC, Baric RS. Amino acid substitutions in the S2 subunit of mouse hepatitis virus variant V51 encode determinants of host range expansion. J Virol 2008;82:1414–24. [PubMed: 18032498]
24. Callison SA, Jackwood MW, Hilt DA. Infectious bronchitis virus S2 gene sequence variability may affect S1 subunit specific antibody binding. Virus Genes 1999;19:143–51. [PubMed: 10541018]
25. Lai SC, Chong PC, Yeh CT, et al. Characterization of neutralizing monoclonal antibodies recognizing a 15-residues epitope on the spike protein HR2 region of severe acute respiratory syndrome coronavirus (SARS-CoV). J Biomed Sci 2005;12:711–27. [PubMed: 16132115]

26. Rudneva IA, Ilyushina NA, Timofeeva TA, Webster RG, Kaverin NV. Restoration of virulence of escape mutants of H5 and H9 influenza viruses by their readaptation to mice. J Gen Virol 2005;86:2831–8. [PubMed: 16186239]

27. Ilyushina N, Rudneva I, Gambaryan A, Bovin N, Kaverin N. Monoclonal antibodies differentially affect the interaction between the hemagglutinin of H9 influenza virus escape mutants and sialic receptors. Virology 2004;329:33–9. [PubMed: 15476872]

28. Coughlin MM, Babcook J, Prabhakar BS. Human monoclonal antibodies to SARS-coronavirus inhibit infection by different mechanisms. Virology. 2009

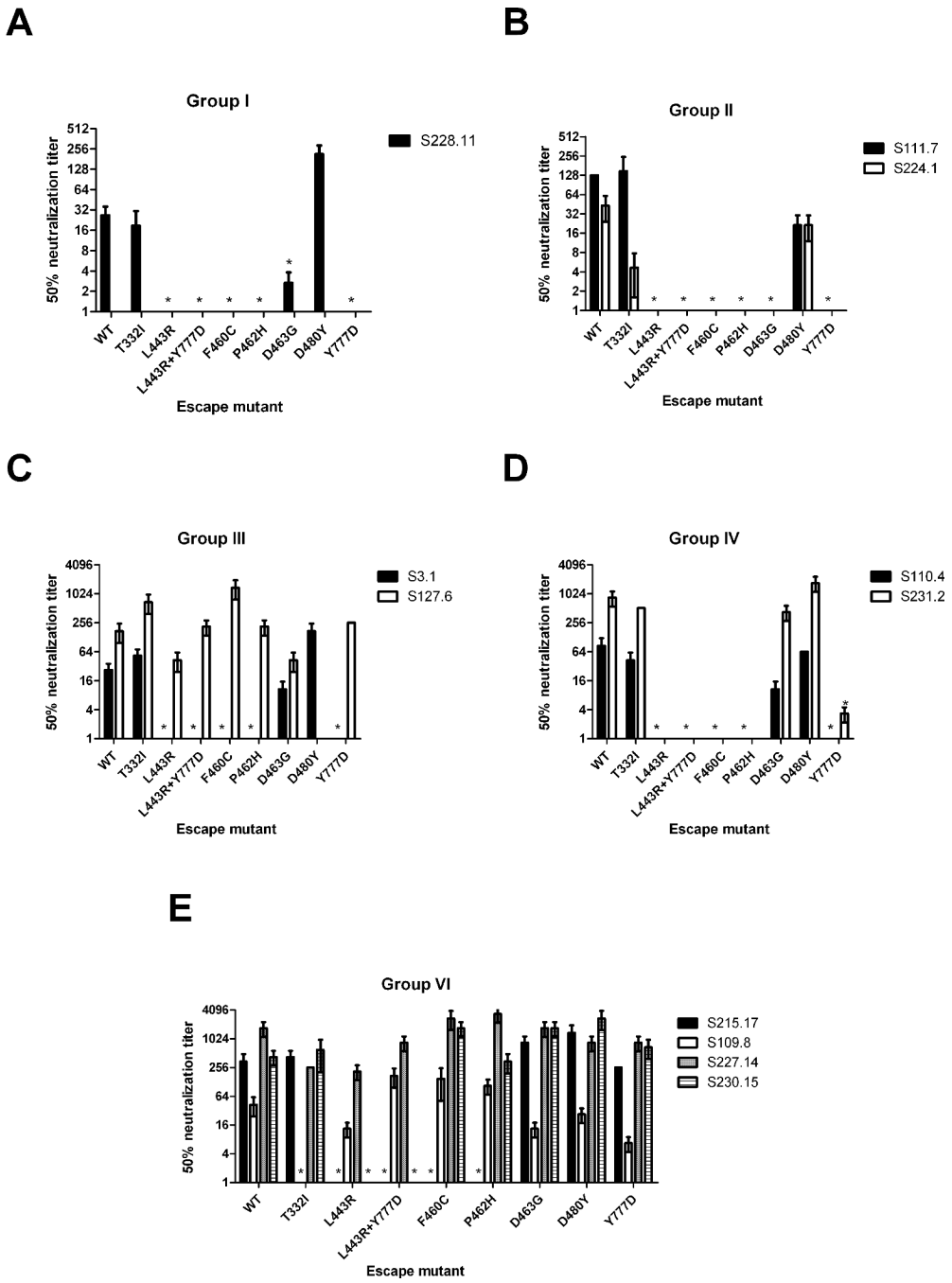

Figure 1.

Neutralization efficacy of wild-type and neutralization-escape mutants by a panel of neutralizing MAbs. Representative MAbs from previously determined neutralization groups I (A), II (B), III (C), IV (D) and VI (E) were tested for their ability to neutralize escape mutants [2]. Starting concentrations of MAbs were selected to show a reduction in neutralization of at least 6 dilutions (1/32); S228.1(6μg/ml), S111.7 (20μg/ml), S224.1 (12μg/ml), S3.1 (2μg/ml), S127.6 (6μg/ml), S110.4 (6μg/ml), S231.2 (20μg/ml), S215.17 (12μg/ml), S109.8 (12μg/ml), S227.14 (40μg/ml) and S230.15 (12μg/ml) as described in materials and methods. MAb dilution at which 50% of the virus was neutralized is plotted. Error bars represent standard deviations. * 2-way ANOVA; $p<0.05$ compared to icUrbani WT.

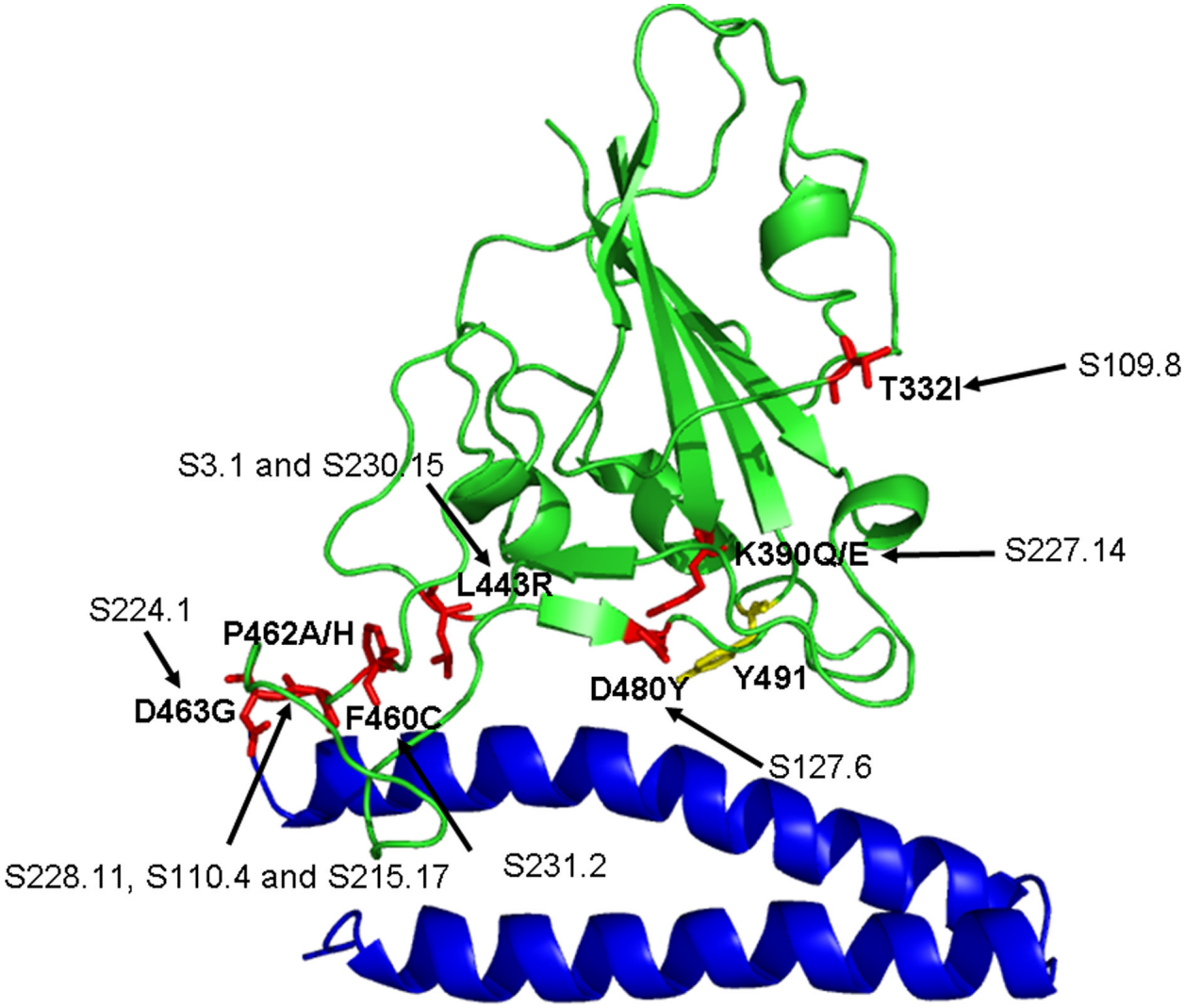

Figure 2.

Locations of neutralization-escape variant mutations on the structure of the SARS-CoV RBD. The location of residues critical for MAb neutralization are mapped onto the strucuture of the SARS-CoV RBD (green) bound to its receptor ACE2 (blue). The a.a. changes associated with neutralization-escape from MAbs S228.11 (P462A/H), S224.1 (D463G), S3.1 (L443R), S127.6 (D480Y), S110.4 (P462H), S231.2 (F460C), S109.8 (T332I), S215.17 (P462H), S227.14 (K390Q) and S230.15 (L443R) are shown in red. Amino acid Y491 (yellow) interacts with multiple residues on the ACE2 molecule.

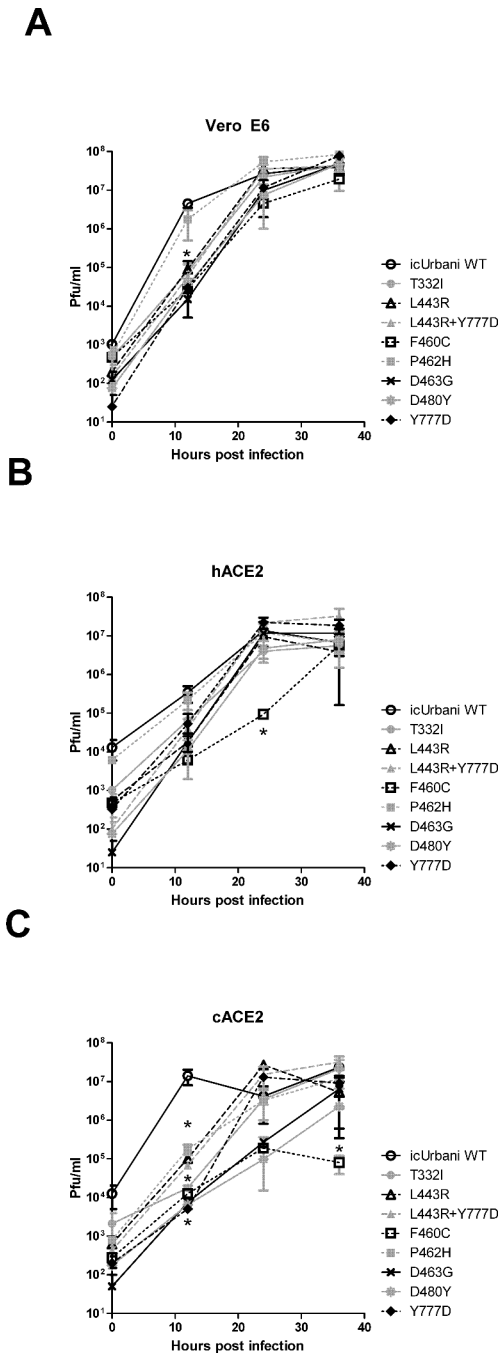

Figure 3.

In vitro growth characteristics of wild type (WT) and neutralization-escape mutant SARS-CoV. Cultures of Vero E6 (A), DBT-hACE2 (B) and DBT-cACE2 (C) cells were infected in duplicate with the icUrbani wild type (icUrbani WT) and neutralization escape mutants T332I (S109.8), L443R (S230.15), L443R+Y777D (S3.1), F460C (S231.2), P462H (S228.11, S110.4, S215.17), D463G (S224.1), D480Y (S127.6) and Y777D (S111.7) at a MOI of 0.1 as described in Materials and Methods. Virus titers at different time points were determined by a plaque assay using Vero E6 cells. Error bars represent standard deviations. * 2-way ANOVA; $p<0.01$ compared to icUrbani WT.

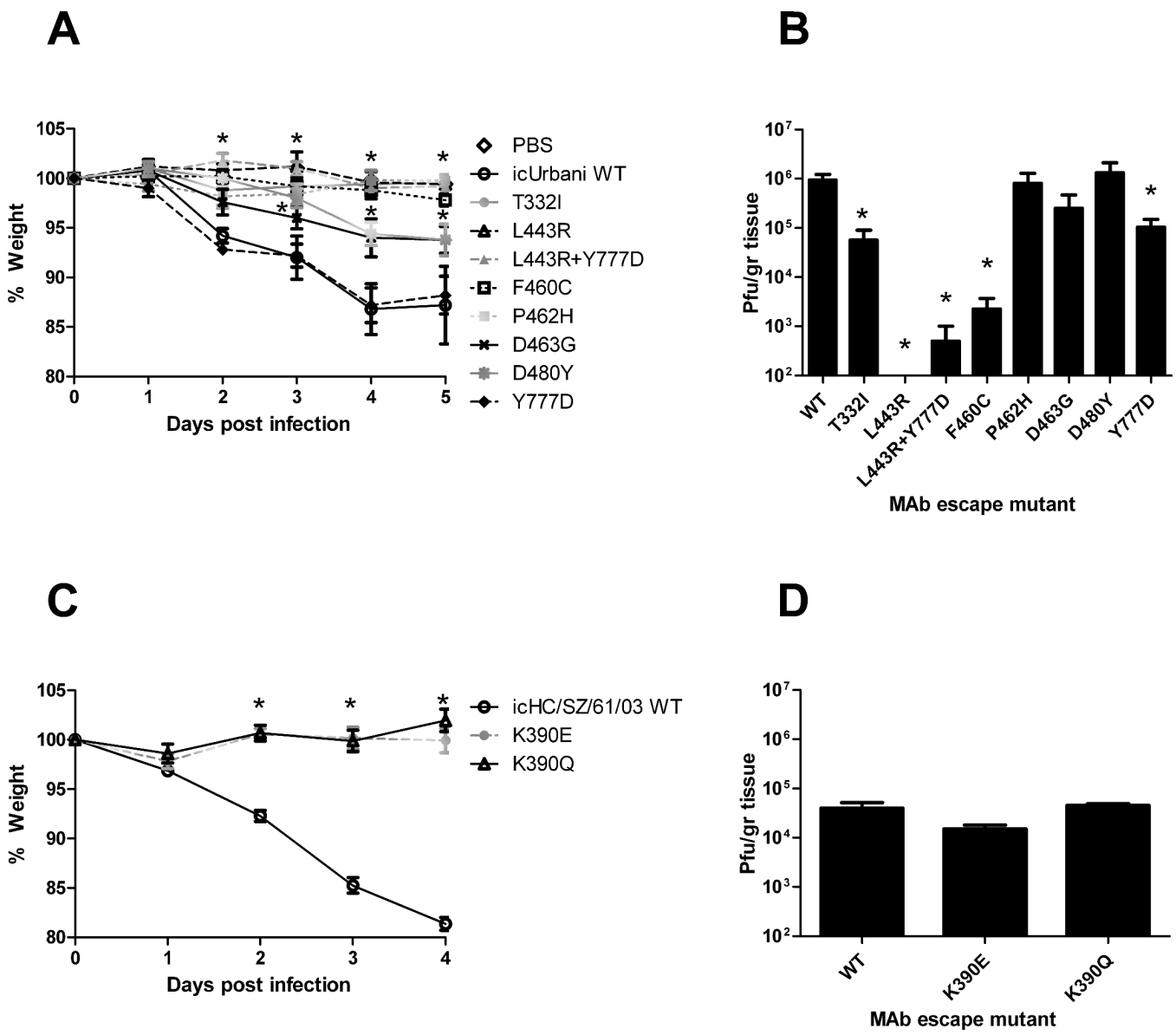

Figure 4.

Effect of neutralization-escape on in vivo replication and morbidity. Weight loss (A and C) and lung titer (B and D) results for 12-month-old female BALB/c mice infected with neutralization-escape mutants T332I (S109.8), L443R (S230.15), L443R+Y777D (S3.1), F460C (S231.2), P462H (S228.11, S110.4, S215.17), D463G (S224.1), D480Y (S127.6) and Y777D (S111.7). Mice were intranasally inoculated with 5×10e5 PFU of the icUrbani strain and its neutralization-escape mutants (A and B) or 10e5 PFU of the icHC/SZ/61/03 strain and its neutralization-escape mutants (C and D) in 50 μl PBS. (A and C) Body weights of infected mice were measured on a daily basis (n = 5 per group). Weight changes are expressed as the mean percent changes for infected animals relative to the initial weights at day 0. (B and D) Lung tissues were harvested from infected mice on day 5 (B) or 4 (D) postinfection and assayed for infectious virus as described in Materials and Methods. Tissue samples from five mice were analyzed at each time point. Error bars represent standard deviations. * 2-way ANOVA; $p<0.01$ compared to icUrbani WT.

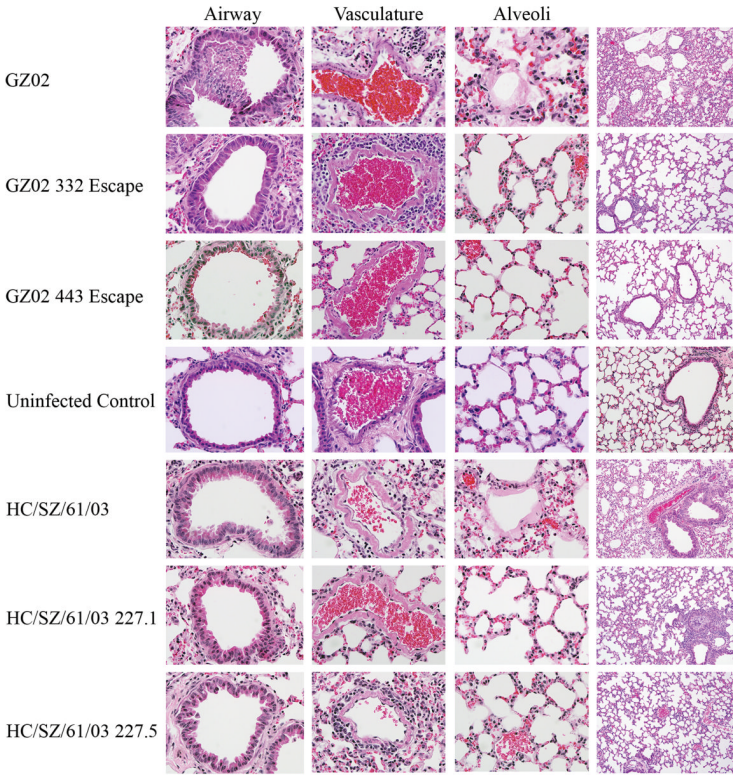

Figure 5.
Lung pathology in 12-month-old BALB/c mice infected with WT and escape mutants of icHC/SZ/61/03 and icGZ02 and sacrificed 5 days post-inoculation. Signs of inflammation and virus induced lung pathology are evident in wild-type infected mice on 4 dpi with necrotizing bronchiolitis. This was accompanied by widespread injury of the alveolar parenchyma consisting of diffuse acute alveolitis, interstitial edema, congestion in the alveolar septa and around small blood vessels, scattered microthrombi in septal capillaries, and hyaline membrane formation. In contrast, mice infected with icGZ02 or icHC/SZ/61/03 neutralization escape mutants showed no inflammation or hyaline membrane formation.

Table 1

Amino acid changes in the SARS-CoV Spike Glycoprotein of neutralization-escape mutants.

Group	MAb	Mutant 1	Mutant 2
I	S228.11	P462A	P462H
II	S111.7	Y777D	Y777D
	S224.1	D463G	Y777D
III	S3.1	L443R+Y777D	L443R+Y777D
	S127.6	D480Y	D480Y
IV	S110.4	P462H	P462H
	S231.2	F460C	F460C
VI	S109.8^	T332I	T332I
	S230.15^	L443R	L443R
	S215.17	P462H	P462H
	S227.14*	K390Q	K390E

^ a.a. changes were observed in neutralization-escape mutants using both icUrbani and icGZ02.

* a.a. changes were observed in neutralization-escape mutants using icHC/SZ/61/03 only.